European Polymer Journal 70 (2015) 18–27

Contents lists available at ScienceDirect

European Polymer Journal

journal homepage: www.elsevier.com/locate/europolj

Hybrid epoxy networks from ethoxysilyl-modified hyperbranched poly(ethyleneimine) and inorganic reactive precursors

Cristina Acebo [a], Xavier Fernández-Francos [a], José-Ignacio Santos [b], Massimo Messori [c], Xavier Ramis [d], Àngels Serra [a,*]

[a] Department of Analytical and Organic Chemistry, Universitat Rovira i Virgili, C/Marcel·lí Domingo s/n, 43007 Tarragona, Spain
[b] Joxe Mari Korta Center, NMR Facility, SGIKER-UPV/EHU, C/Tolosa Hiribidea, 72, 20018 Donostia, Spain
[c] Università degli Studi di Modena e Reggio Emilia, Dipartimento di Ingegneria "Enzo Ferrari", Via P. Vivarelli 10, 41125 Modena, Italy
[d] Thermodynamics Laboratory, ETSEIB Universitat Politècnica de Catalunya, Av. Diagonal 647, 08028 Barcelona, Spain

ARTICLE INFO

Article history:
Received 8 May 2015
Accepted 24 June 2015
Available online 25 June 2015

Keywords:
Hyperbranched polymers
Epoxy resin
Sol–gel
Coatings
Hybrids

ABSTRACT

New epoxy–silica hybrid coatings were prepared by a dual process consisting of a sol–gel process using tetraethoxysilane (TEOS) or 3-glycidyloxypropyl trimethoxysilane (GPTMS) in the presence of hyperbranched poly(ethyleneimine) with ethoxysilyl groups at the chain ends (PEI-Si) followed by a homopolymerization of diglycidylether of bisphenol A (DGEBA) using 1-methylimidazole (1-MI) as anionic initiator. The influence of the amount of TEOS and GPTMS in the characteristics of the coating was examined.

Thin transparent films were obtained and their morphology was observed by transmission electron microscopy (TEM). The hydrolytic condensation was confirmed by ^{29}Si NMR studies. Cage-like nanometric structures were formed in case of adding GPTMS and bigger silica particles on adding TEOS to the formulation. Thermal stability was evaluated by thermogravimetry and the scratch resistance properties were also investigated, showing an improvement in resistance to break and to detachment in all the coatings containing GPTMS.

1. Introduction

Hybrid organic/inorganic nanomaterials have attracted a great deal of attention in the field of polymer research as well as in industrial applications because their advanced properties like abrasion and scratch resistance, toughness, mechanical properties, self-healing or corrosion resistance attributed to the formation of the inorganic particles in the polymer matrix, while keeping transparency [1–4].

Hybrid materials are usually obtained by the addition of preformed nanoparticles, the most significant examples being layered silicates, silica nanoparticles or polyhedral oligomeric silsesquioxane (POSS) [5–7]. In these cases, the homogenous dispersion of the silica filler in the organic matrix may represent a challenge. An alternative route to incorporate silica into the polymer matrix is the sol–gel process involving a series of hydrolysis and condensation reactions under mild conditions starting from hydrolyzable multifunctional alkoxysilanes as inorganic precursors for forming inorganic domains, being tetraethoxysilane (TEOS) the most typical one [8–12]. Using this route it is possible to grow an inorganic phase into an

* Corresponding author.
E-mail address: angels.serra@urv.cat (À. Serra).

http://dx.doi.org/10.1016/j.eurpolymj.2015.06.029
0014-3057/

organic matrix allowing a fine dispersion of the inorganic phase even at molecular level. Another advantage of the *in situ* generation of the inorganic phase is that the addition of a small amount of nanoparticles drastically increases the viscosity, which is always an important issue in coatings applications whereas the formulation applied before the sol–gel process still has a low viscosity [13].

Hyperbranched polymers (HBP)s have been applied as modifiers in epoxy thermosets to improve toughness [14–16]. In the last years, they have been extensively used because of their special architectures present some advantages over conventional toughening agents. HBPs help to keep the viscosity of the formulations at a reduced value due to the lower entanglement caused by the branching, whereas they do not produce any appreciable decrease in thermomechanical parameters. The highly branched structures give access to a large number of functional end groups and thus allow tailoring the compatibility/reactivity of the HBPs in the resin resulting in homogeneous or phase separated materials [17,18]. Due to the enhancement of the thermomechanical properties that can be achieved by adding HBPs and the improvement in nanocomposite processing reached through sol–gel procedures, the strategy of combining both methodologies was adopted by several authors [19–21].

Inorganic domains can be generated from organoalkoxy silane precursors with functional groups (epoxy, amine, etc.), which are used as coupling agents, to react with organic matrices enabling a good incorporation of inorganic structures into an organic phase [22,23]. In this way, phase separation in organic and inorganic domains can be prevented by the use of these compounds, being one of the most used in epoxy matrices 3-glycidoxypropyltrimethoxysilane (GPTMS) [24]. Thus, it seems that the preparation of multifunctional coupling agents by silylation of the end groups of hyperbranched polymers can be greatly advantageous to improve the properties of epoxy resins by generation of silica-like particles by sol–gel process from the alkoxysilane end groups. Sangermano et al. [19] prepared epoxy–silica materials using as inorganic precursor hyperbranched aromatic–aliphatic polyester modified to different extents at the final phenol groups by reacting with 3-isocyanatepropyl triethoxysilane. The addition of ethoxysilyl-modified HBP as a coupling agent allowed the covalent bonding of inorganic and organic networks. In some cases, TEOS was also added to the formulation. The authors could clearly demonstrate that the use of the silylated hyperbranched polymer was advantageous in the formation of transparent films in contrast to what occurred by applying the same curing procedure without silylated hyperbranched but adding TEOS as source of silica particles.

In our group, we synthesized a triethoxy silylated hyperbranched poly(ethylene imine) (PEI-Si) which was used in different proportions as inorganic precursor in diglycidylether of bisphenol A (DGEBA) formulations using 1-methylimidazole as anionic curing agent [25]. The materials obtained were highly transparent and no particles could be observed by TEM analysis. However, ^{29}Si NMR spectra demonstrated that the sol–gel processes occurred with the formation of cage-like structures (POSS) with particle size <10 nm. One of the peculiarities of these hybrid coatings was the increase in surface hardness due to the presence of silica domains well dispersed in the epoxy matrix and formulations with intermediate PEI-Si had the highest resistance to penetration. It has been reported that the incorporation of POSS cages into polymers improves several properties such as thermal stability, glass transition temperature, flame and heat resistance and modulus [26].

In spite of the good characteristics of the hybrid materials obtained in our previous study, there was not a clear evidence of a real covalent linkage between PEI-Si structure (and the POSS cages formed by sol–gel) with the epoxy matrix, which is usually required to achieve the best mechanical performance in sol–gel thermosets. Because of that, in the present work we have taken the formulation with DGEBA/PEI-Si 50:50 w/w as the neat material and we have studied the effect of adding different proportions of TEOS or GPTMS. The addition of TEOS aims at increasing the particle size and the addition of GPTMS to enhance the interaction between organic and inorganic phases. In addition, the presence of a single epoxy group in the GPTMS structure would produce a looser epoxy network structure. We have also tested if there is a synergistic effect of adding both silicon precursors to the selected formulation. The characterization of the materials has been performed by ^{29}Si NMR spectroscopy in solid state and the morphology of the hybrid was visualized by TEM microscopy. The mechanical properties of the films were rated by scratch tests.

2. Experimental

2.1. Materials

Polyethyleneimine (PEI) Lupasol®FG (PEI800, 800 g/mol, BASF) was dried under vacuum before use. 1-Methylimidazole (1-MI) and tetraethyl orthosilicate (TEOS) were purchased from Sigma-Aldrich and used without further purification. Chloroform was purchased from Scharlab, dried under $CaCl_2$ and distilled before used. Diglycidylether of bisphenol A (DGEBA) Araldite GY 240 (EEW = 182 g/eq) was gently provided by Huntsman. Ammonium dihydrogen phosphate ($NH_4H_2PO_4$), 3-isocyanatepropyl triethoxysilane (TESPI) and 3-glycidoxypropyl trimethoxysilane (GPTMS) were purchased from Acros Organics. Triethoxysilyl modified hyperbranched poly(ethyleneimine) (PEI-Si) was prepared as described previously [25] by reacting Lupasol and TESPI in chloroform.

2.2. Sample preparation

In all the samples the weight proportion of PEI-Si/DGEBA was 50:50 and 2 phr of 1-MI in reference to the DGEBA were added. The inorganic precursors TEOS and GPTMS were added to the formulations in the range between 10 and 40 wt%. The

formulations were coated on glass slides by means of a wire-wound applicator. The sol–gel process was carried out by thermal treatment at 80 °C for one day in a controlled highly humid atmosphere (95–98% relative humidity controlled by a saturated solution of aqueous $NH_4H_2PO_4$) and was followed by a thermal curing process at 150 °C during 2 h in an oven.

2.3. Characterization techniques

Solution NMR spectra were carried out in a Varian Gemini 400 spectrometer using $CDCl_3$ as the solvent. For ^{29}Si NMR measurements tetramethylsilane (TMS) was used as the reference. For ^{29}Si NMR measurements the conditions used were d_1 = 0.4 s acquisition time = 0.7 s, a number of scans of 3000 and applying an inverse gated decoupling pulse sequence.

Solid-state ^{29}Si CPMAS NMR spectra were recorded on a Bruker AVANCE III 400 MHz spectrometer WB equipped with wide bore 9.4 *T* superconducting magnet in Larmor frequencies of 79.5 MHz. Powdered samples were packed into 4 mm ZrO_2 rotors. Chemical shifts are given relative to TMS. NMR spectra were registered using a CP MAS pulse sequence with an acquisition time of 0.0184 s and 34,432 scans using the following parameters: rotor spin rate 10,000 Hz and recycling delay of 5 s. In the processing of the data exponential apodization with line broadening 40 Hz, FT and manual phasing and baseline correction were used.

Calorimetric analyses were carried out on a Mettler DSC-822e thermal analyzer. Samples of approximately 10 mg were placed in aluminum pans under nitrogen atmosphere. The calorimeter was calibrated using an indium standard (heat flow calibration) and an indium-lead-zinc standard (temperature calibration). T_gs of the hybrid materials were determined at a heating rate of 30 °C/min after a first scan from 0 to 180 °C followed by cooling at 10 °C/min from 180 °C/min to 0 °C. The error is estimated to be approximately ± 1 °C.

Thermogravimetric analyses were carried out in a Mettler TGA/SDTA 851e thermobalance. Samples with an approximate mass of 8 mg were degraded between 30 and 900 °C at a heating rate of 10 °C/min in air (100 cm^3/min measured in normal conditions).

The morphology of the different hybrids was analyzed by imaging thin pieces from the samples. These pieces had a thickness of 60 μm, in a transmission electron microscope (TEM, JEOL model 1011) with a 0.2 nm resolution.

Scratch test was carried out on a CSM Micro-Combi Tester by using Rockwell 0.1 mm diameter spherical diamond indenter. Progressive scans increasing the normal load from 10 to 5000 mN were made for a scratch length of 3 mm and at a scratch rate of 60 mm min^{-1}, according to an adaptation of the Test Mode A described by the technical standard ASTM D 7027. A prescan with a constant and very low load (10 mN) was carried out in order to record the starting surface profile. At least 5 progressive scans were performed for each sample with penetration depth (P_d) recording. First and second critical load values (Lc_1 and Lc_2) were determined by optical microscopy after scratch test evaluating the occurrence of the first visible crack on the coating surface and the detachment of the coating from the glass substrate, respectively.

3. Results and discussion

The synthesis of the triethoxysilylated hyperbranched poly(ethyleneimine) (PEI-Si) was conducted following the procedure described in a previous work [25]. All the primary and secondary amines were modified by using TESPI. By ^{29}Si NMR spectroscopy two signals were observed at −45.4 and −45.0 ppm attributable to the silyl groups attached to the primary and to the secondary amines at the HBP structure. Scheme 1 shows the idealized structure of the PEI-Si together with the other compounds used in the formulations.

3.1. Preparation of films from DGEBA and PEI-Si and TEOS or GPTMS mixtures

The hybrid materials were prepared using the same protocol as the previous work [25], which is based in two well-known processes: sol–gel and epoxy anionic homopolymerization. Both processes partially overlapped because of the easy thermal homopolymerization of epoxides initiated by 1-MI, even at moderate temperatures. 1-MI also acts as basic catalyst in the sol–gel process together with tertiary amine groups located in the PEI-Si structure. The use of acidic conditions is prevented by the basic character of the HBP [2]. It has been reported that sol–gel processes under basic conditions lead to the formation of particulate inorganic domains, due to the fast rates of condensation reactions that leads to separation by nucleation and growth mechanism [24]. Water dissociates to produce nucleophilic hydroxyl anions in a quick first step. The hydroxyl anions lead to an SN_2 substitution on silicon atom to produce the corresponding silanol [27].

While sol–gel process produces inorganic structures, epoxy homopolymerization originates the networked organic matrix. The interaction between PEI-Si and the organic matrix could not be confirmed in the previous study, since all the primary and secondary groups of PEI were transformed into ureas by reaction with TESPI. Neither urea groups nor tertiary amines are sufficiently nucleophilic to attack epoxides in an extensively way. However, a partial interaction by hydrogen bonding was foreseeable. To increase the interaction between both domains, in the present study we have added GPTMS, which has an epoxy group that can homopolymerize and a methoxysilylated group that can participate in the formation of cage-like particles with ethoxysilyl groups from PEI-Si. The addition of TEOS has the aim to create bigger inorganic particles and to increase the proportion of Si in the materials, reducing the proportion of cage-like structures, since the higher

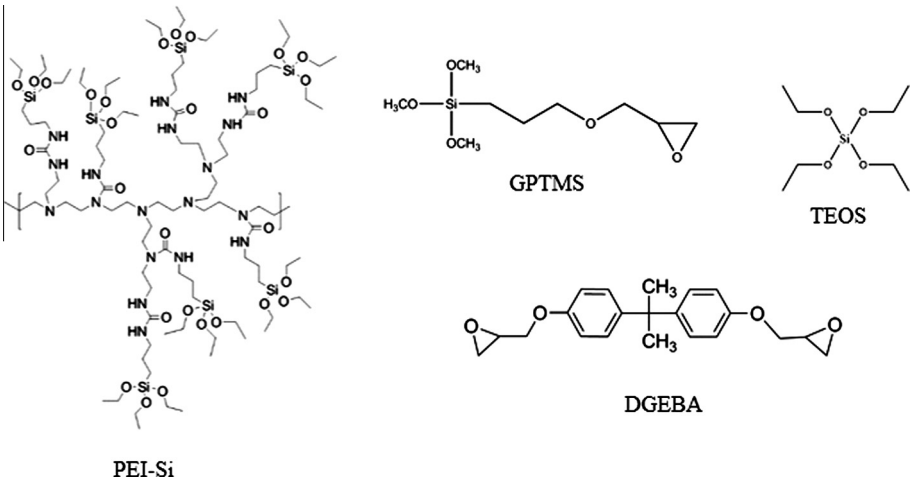

Scheme 1. Idealized structure of the ethoxysilylated poly(ethyleneimine) prepared and structure of the compounds used in the preparation of the hybrid thermosets.

Table 1
Notation and compositions of the formulations studied. All the formulations have 2 phr of 1-MI in reference to DGEBA.

Formulation	DGEBA		PEI-Si		TEOS		GPTMS	
	wt (%)	mol (%)	wt (%)	mol (%)	wt (%)	mol (%)	wt (%)	mol (%)
Neat	50	96	50	4	–	–	–	–
10% TEOS	45	80.4	45	3.5	10	16.1	–	–
20% TEOS	40	67.5	40	3.1	20	29.4	–	–
30% TEOS	35	56.2	35	2.4	30	41.4	–	–
40% TEOS	30	45	30	2	40	53	–	–
10% GPTMS	45	82.5	45	3.5	–	–	10	14
20% GPTMS	40	71.1	40	3	–	–	20	25.9
30% GPTMS	35	58	35	2.5	–	–	30	39.5
40% GPTMS	30	47.4	30	2	–	–	40	50.6
20% TEOS/20% GPTMS	30	48	30	2	20	24	20	26

functionality of TEOS can lead to networked silica particles and bicontinuous nanocomposites. The addition of TEOS and GPTMS at the same time aims at obtaining larger particles covalently linked to the epoxy network.

Table 1 collects the composition of all the formulations studied in weight percentages.

The sol–gel hybrid films were easily prepared by mixing the different proportions of the components of the formulation and adding 2 phr of 1-MI (parts of amine per hundred parts of DGEBA) obtaining in all cases homogeneous mixtures. The viscous mixtures were coated on glass slides and then heated for one day at 80 °C in a controlled high humidity atmosphere. After sol–gel process the coatings were solid and transparent and the condensation reaction and the curing of DGEBA were then performed in an oven at 150 °C during 2 h. The films obtained after this schedule were hard and transparent with a light color and without any visible particle at the naked eye (see Fig. 1). The optical quality based on the transparency of the materials prepared accounts for the formation of small inorganic domains with sizes lower than 400 nm. Although some shrinkage stress should occur due to the significant volume change caused by the loss of alcohol and water, no cracks, voids or debonding were observed.

3.2. Characterization of sol–gel condensed films

To confirm the formation of inorganic structures by condensation of silanols, ^{29}Si NMR studies of the cured samples were registered in the solid state. Fig. 2 shows the ^{29}Si CPMAS NMR spectra of the material obtained from formulations 30% GPTMS and 30% TEOS.

It should be commented that no signals corresponding to the silicon precursors were observed in any spectra. Both spectra containing GPTMS or TEOS show peaks in the region of T_i units. For the sample 30% GPTMS the maximum of the T peak is −69 ppm which can be assigned to T_3 of cubic cage-like structures according to the reported by Matejka et al. [28] for sol–gel processes from compounds having trialkoxysilyl groups. They described that cyclization is a typical feature of the polymerization of alkoxysilanes. The trifunctionality of the PEI-Si in the 30% TEOS sample also contributes to the formation of T_3 units in addition to the Q_i units produced according to the tetrafunctionality of TEOS. However, in the sample with TEOS the

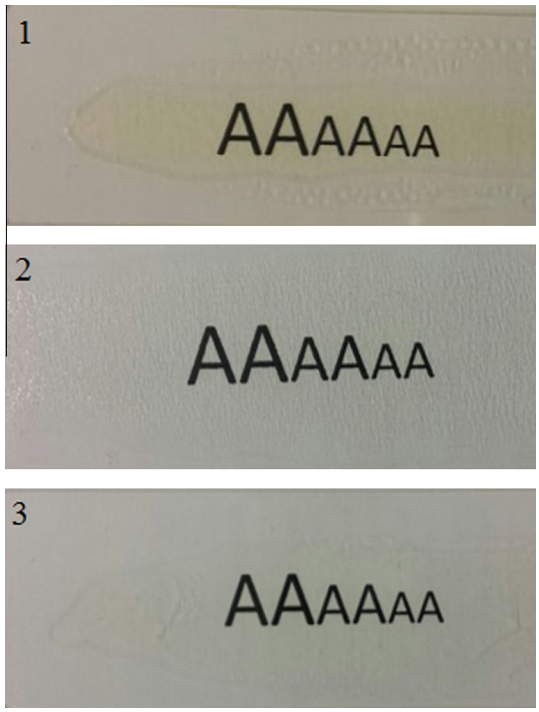

Fig. 1. Photographs of the films prepared showing the transparency and appearance. (1) Neat material; (2) 40% TEOS and (3) 40% GPTMS.

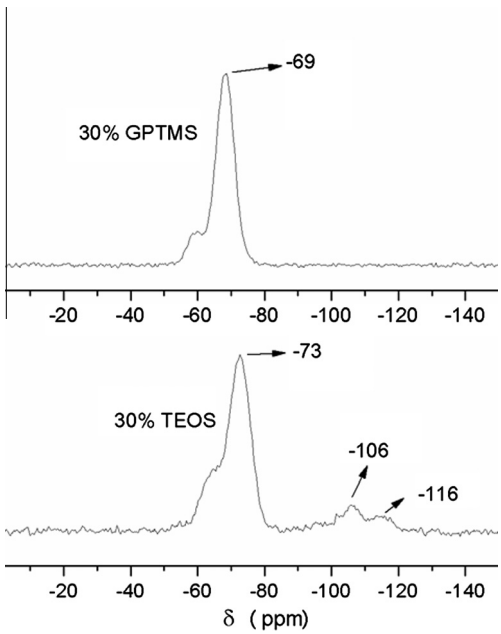

Fig. 2. ^{29}Si CPMAS NMR spectra of the hybrid thermosets obtained from formulations 30% GPTMS and 30% TEOS.

maximum of the peak is shifted to high field in 4 ppm. This fact could be explained by the formation of linear T_3 structures or cages with a high number of silicon atoms per structure because of the reaction with TEOS. Cubic cage-like structures reduce the valence angles of Si atoms and consequently the density of positive charge diminishes. Thus, in linear structures or in bigger cages the internal tension is reduced and the signal would be high-field shifted [28].

The apparition of a shoulder at higher chemical shift in both spectra can be attributed to the presence of T_2 units, with uncondensed silanols or to the incompletely condensed POSS cages. This shoulder seems to be proportionally more intense

Table 2
Thermal data of the hybrid materials prepared obtained by TGA and DSC.

Formulation (DGEBA/PEI-Si)	T_g[a] (°C)	$T_{5\%}$[b] (°C)	$T_{1st\ peak}$[c] (°C)	T_{max}[d] (°C)	$T_{3rd\ peak}$[e] (°C)	Residue[f] (wt%)	Residue[g] (wt%)
Neat	89	254	267	371	562	8.41	9.10
10% TEOS	83	254	268	372	562	10.1	10.27
20% TEOS	82	255	267	371	557	11.08	11.74
30% TEOS	78	254	267	373	562	12.84	13.1
40% TEOS	75	254	266	375	570	13.5	14.24
10% GPTMS	73	252	263	364	560	9.36	9.67
20% GPTMS	68	254	262	365	574	10.26	10.75
30% GPTMS	68	256	258	366	610	11.62	12.30
40% GPTMS	67	259	259	367	610	12.30	13.62
20% TEOS/20% GPTMS	68	257	268	368	576	12.49	13.24

[a] Glass transition temperature of the hybrid materials.
[b] Temperature of the onset decomposition on TGA data at 10 °C/min taken as the 5% weight loss.
[c] Temperature of the maximum rate of the first degradation peak.
[d] Temperature of the maximum decomposition rate.
[e] Temperature of the maximum rate of the third degradation peak.
[f] Experimental residue at 900 °C in air atmosphere.
[g] Theoretical residue.

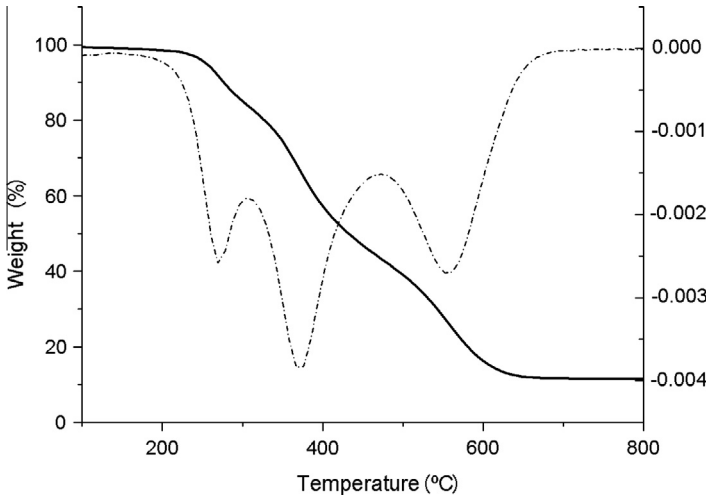

Fig. 3. TGA and DTG curves of the material obtained from the formulation with a 20% TEOS in air atmosphere.

for the TEOS sample. In the spectrum of the material containing TEOS, Q signals can be observed in the region of 100–120 ppm. The signals are broad and have a bad resolution but Q_3 signals at −106 ppm are more intense than Q_4 at −116 ppm, indicating that the condensation of TEOS has not been completed. The assignment of signals is based on previously reported results [28,29].

3.3. Thermal characterization

Calorimetric studies allowed determining the T_g of the hybrid materials. The values are collected in Table 2. The T_g of the neat formulation, obtained only from the ethoxysilyl-modified HBP and DGEBA is of 89 °C. Assuming that the organic phase consists mainly of homopolymerized DGEBA, this is a rather low value in comparison with those reported in the literature [30,31] One must take into account that, during the sol–gel process, the sample is exposed to a highly humid environment, and that ethanol and water are released by the hydrolysis and condensation of ethoxysilyl groups. Both ethanol and water can participate in the anionic homopolymerization of DGEBA as chain-transfer agents, reducing the crosslinking density and consequently the T_g [32]. The hyperbranched structure of the ethoxysilyl modifier is flexible, but it is assumed that it is mainly embedded and immobilized into the inorganic domains. However, it might be that some flexible segments resulting from incomplete hydrolysis and condensation might have an effect on the organic phase.

On increasing the proportion of TEOS in the formulation the T_g values slightly decrease. This result follows the opposite trend to that reported by Sangermano et al. [19]. They observed an increase of 20–45 °C on adding a 30% of TEOS to hyperbranched silylated modified HBP epoxy formulations. However, a decrease in the T_g was reported by Matejka et al. [33] on

adding TEOS to an epoxy–amine formulation. These authors attributed the reduction in T_g to a non-efficient immobilization of the epoxy network by silica, due to the low extent of the covalent interfacial bonding. As we will demonstrate by TEM, the addition of a high proportion of TEOS to the formulation leads to a clear separation into large inorganic domains, which do not influence greatly the mobility of the organic network. Finally, as we saw by ^{29}Si NMR spectroscopy, TEOS is not fully condensed, since Q_3 signals seems to be predominant to Q_4. The low conversion in the sol–gel process results in the formation of undercured soft flexible silica/siloxane domains leading to plasticization of the material resulting in a decrease in the T_g [33].

The addition of GPTMS to the formulation also leads to a reduction of the T_g values much noticeable than on adding similar proportions of TEOS. The replacement of DGEBA by the monofunctional epoxide GPTMS leads to a decrease in the average epoxide functionality and a reduction of the epoxy network crosslinking density. In addition, the flexible structure of GPTMS can cause a certain plasticization. Such effects lead to the corresponding diminution of the T_g as it was reported previously [33]. Sun et al. [34] compared the effect of adding micro or nanofillers in epoxy composites and observed that on increasing the proportion of nanoparticles the T_g of the nanocomposite is reduced whereas the contrary trend was observed for microparticles. This observation helps to understand how the formation of a higher proportion of inorganic nanostructures reduces the T_g as observed. The material obtained from a mixture with a 20% of TEOS and a 20% of GPTMS shows the same T_g than the one measured for the 20% GPTMS material, without any further reduction for the presence of TEOS in the sample.

The thermal stability of the materials prepared was studied by thermogravimetry. In Fig. 3 the weight loss and the derivative of the degradation curve are represented for the material 20% TEOS.

It should be commented that all the degradation curves of the materials showed a similar shape, with three defined processes, but no loss of volatiles was observed at low temperature which indicates that the condensation of silanol groups was practically complete. The first degradation peak corresponds to the degradation of poly(ethyleneimine) structure [31], the second peak to the degradation of the epoxy network, whereas the third corresponds to the oxidative degradation leading to the loss of organic matter giving rise to the silicon residue [25].

The data obtained from the degradation curves are collected in Table 2. As we can see, the addition of TEOS or/and GPTMS to the formulation does not lead to any effect in the initial temperature of degradation, taken as the 5% of weight loss. The temperatures of the maximum of the three degradative processes are very similar with the exception of the temperature of the third peak for samples with GPTMS that shifts to higher temperatures with the increasing amount of this coupling agent. That could be explained by the increase in the covalent bonding between organic and inorganic structures. The residue at 900 °C as expected increases with the amount of Si in the material. On comparing the calculated Si content with the experimental residue we can see that there are not great differences, but the experimental values are slightly lower than those calculated. It can be related to an incomplete hydrolysis of alkoxide groups that was reflected in the presence of T_2 and Q_3 signals in the ^{29}Si NMR spectroscopy.

3.4. TEM analysis

Fig. 4 shows the TEM micrographs of some of the hybrid materials prepared. In the micrographs the difference in the electronic transmission between organic and inorganic phases allows assign the dark area to the Si particles, covalently connected to the organic matrix. As in the previous paper [25], in the micrograph of the neat material we cannot see any appreciable aggregation between inorganic particles in the matrix by the presence of the cage-like structures obtained by

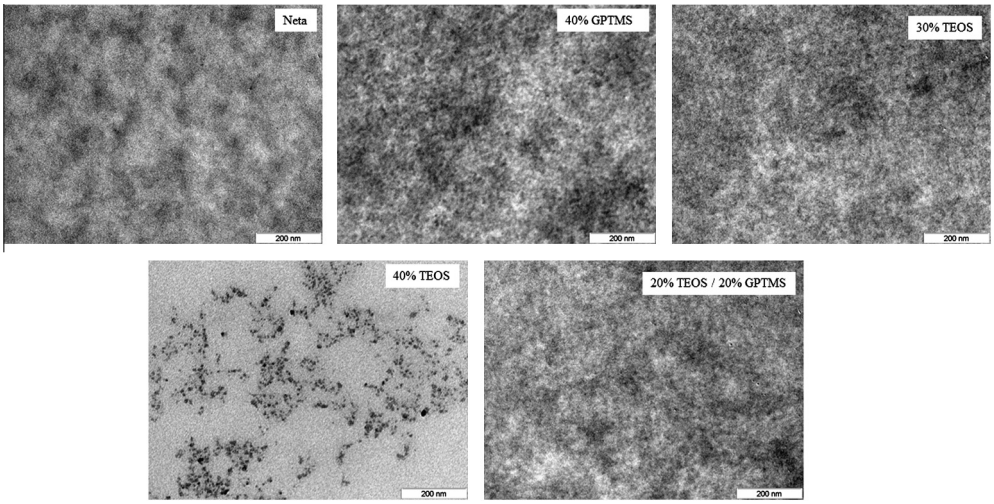

Fig. 4. TEM micrographs of hybrid materials obtained from different formulations at a magnification of 120 K.

sol–gel from ethoxysilylated PEI and DGEBA. The POSS particles formed are embedded in the epoxy matrix with sizes <10 nm that rends transparency to the hybrid coating.

On increasing the proportion of POSS structures the nanodomains become interconnected and a bicontinuous nanophase-separated morphology can be observed in the micrograph of the sample 40% of GPTMS which shows a more inhomogeneous morphology with less-defined boundaries between domains. A similar behavior was observed in epoxy thermosets modified with POSS end-capped polyesters [35].

On adding a proportion of TEOS up to 30% to the formulation, the material obtained presented no clear evidence of the formation of silica particles and a morphology similar to the 40% GPTMS material is observed in Fig. 4. However, on increasing the proportion of TEOS up to 40% clear aggregates of silica particles with particle sizes less than 40 nm can be observed. The material containing 20% of TEOS and 20% of GPTMS shows a similar morphology that the one commented for 40% GPTMS. Although the generation of particles with TEOS or GPTMS is different because of the tetrafunctionality of the former and the trifunctionality of the latter, the Si content for both formulations is similar. Thus, it seems that in our systems the morphology of the material is more dependent on the Si content than on the structure of the silica precursor. However, the presence of the PEI-Si structure in all those materials helps dispersing the particles in the matrix, leading to a more homogeneous distribution.

3.5. Scratch resistance analysis

One of the main ways to improve scratch resistance in organic coatings is to reinforce them by embedding fillers in the organic matrix. To reach significant improvements the regular distribution and the dispersion of the particles into the matrix is crucial. Therefore, to increase scratch resistance, the *in situ* formation of the inorganic nanodomains through sol–gel processes has been demonstrated as one of the best strategies [36]. Some of the data extracted from scratch test are collected in Table 3.

Penetration depth values (P_d) can be considered as an indication of the resistance to penetration which includes rigidity (modulus) and hardness. These values can be affected by structural parameters of the organic network structure and inorganic domains and the lowest values represent the highest resistance to penetration during scratching. From both series of results detected at 1N and 4N of normal load reported in the table we can see that the presence of TEOS in the hybrid coating keeps the resistance to penetration in reference to the neat material whereas the addition of GPTMS reduces this characteristic. The lower functionality of GPTMS could explain this behavior, since the flexibility increases (that is the modulus decreases) due to a reduction of crosslinking density as it was noted by the decrease in the T_g.

The scratch behavior of coatings is the result of a complex interrelation among several parameters and factors such as modulus, strength, friction coefficient, thickness and viscoelasticity of the coating and its adhesion to the specific substrate [37]. The scratch resistance properties of the hybrid coatings here investigated can be evaluated by first and second critical load values (Lc_1 and Lc_2, respectively) reported in Table 3. Lc_1 (normal load at which the first crack appears on the surface) can be seen as an indirect indication of cohesive forces (strength and deformability) in the coating material and represents the main parameter for the evaluation of the scratch resistance. Lc_2 (normal load at which the detachment of coating from substrate occurs) is an indirect indication of adhesive forces between coating and substrate. In the present case Lc_1 and Lc_2 values are affected by very high values of standard deviation (not reported in table but up to 300 mN in some cases) suggesting a general inhomogeneity of the coating from a mechanical point of view. In this view, Lc_1 values indicate a comparable resistance to scratch for all the coatings investigated (with the negative exception of 30% TEOS sample). It has to be noticed that the addition of GPTMS to the formulation leads to more reliable Lc_1 values (lower standard deviation values), which seems to indicate a more homogeneous material. An optimum Lc_1 is achieved with 40% of GPTMS. More interestingly, Lc_2 values offer a significant differentiation among the different series of coatings. The presence of TEOS induces a slight improvement of the detachment resistance of the coatings (with the exception of 10% TEOS sample) while the presence

Table 3
Data from scratch tests of the hybrid coatings prepared.

Formulation	P_d 1N[a] (μm)	P_d 4N[a] (μm)	Lc_1[b] (mN)	Lc_2[c] (mN)
Neat	10.1 ± 0.3	31.6 ± 0.2	670	3530
10% TEOS	10.1 ± 0.9	30.7 ± 2.5	800	3000
20% TEOS	10.9 ± 1.7	35.9 ± 6.7	560	3740
30% TEOS	9.8 ± 1.7	28.8 ± 0.7	260	3840
40% TEOS	10.5 ± 1.2	30.5 ± 0.8	430	3730
10% GPTMS	16.3 ± 2.7	46.2 ± 2.2	650	Not detected
20% GPTMS	12.4 ± 0.4	39.8 ± 2.6	680	Not detected
30% GPTMS	16.1 ± 1.0	45.1 ± 1.1	620	Not detected
40% GPTMS	16.2 ± 1.6	48.9 ± 4.1	820	Not detected
20% TEOS/20% GPTMS	11.9 ± 3.6	36.3 ± 8.2	450	Not detected

[a] Penetration depth values recorded at 1N and 4N of normal load.
[b] First critical load.
[c] Second critical load.

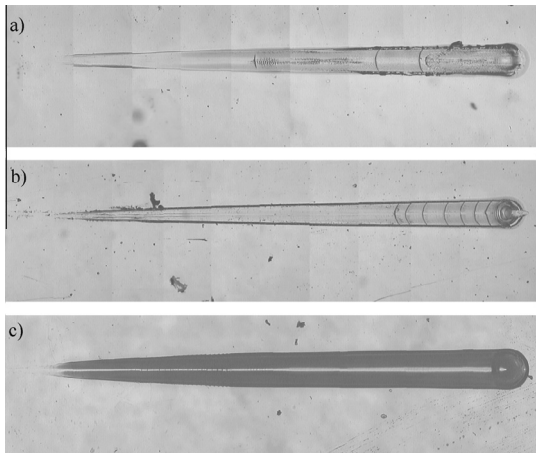

Fig. 5. Optical micrographs after scratch test of (a) Neat, (b) 20% TEOS and (c) 20% GPTMS materials.

of GPTMS in the formulation produces an extremely adhesive coating with absence of detectable second critical load values in the experimental conditions used for the test.

Some representative optical micrographs after scratch test are collected in Fig. 5. The presence of a second critical load Lc_2 is well evident in the case of Neat and 20% TEOS coating formulations (Fig. 5a and b, respectively) as indicated by the arc tensile cracks shown to the right part of the scratch. On the contrary, a second critical load Lc_2 is not shown by the system containing GPTMS (Fig. 5c).

4. Conclusions

The addition of GPTMS to the formulation led to materials with a high transparency by the formation of cage-like structures that also incorporates the final groups of the PEI-Si structure. This was confirmed by CPMAS ^{29}Si NMR spectroscopy. The materials obtained showed a slightly lower T_g due to a reduction in the crosslinking density of the organic domain. The modified materials presented a similar thermal stability than the neat formulation although the last thermo oxidative process is delayed, which was attributed to the covalent linkage of inorganic particles to the epoxy matrix. The observation of these materials by TEM revealed that nanodomains became interconnected with the formation of a bicontinuous nanophase-separated morphology. The penetration depth, measured by scratch tests, increased on increasing the proportion of GPTMS in the formulation according to a lower rigidity by the reduction in crosslinking density.

When TEOS was added to the formulation, the ^{29}Si NMR spectra showed, in addition to T signals, corresponding to cubic-like structures, broad and unresolved Q signals attributed to complete and incomplete TEOS condensation. T_g values are slightly reduced by the addition of TEOS. In TEM microscopy the presence of 40% TEOS in the hybrid material led to the observation of well separated silica particles.

The addition of GPTMS or TEOS to the formulation did not increase the overall scratch characteristics in reference to the neat material, since cage-like structures were already produced by the sol–gel condensation of ethoxysilylated PEI. However, the scratch tests confirmed the higher homogeneity of the materials modified with GPTMS due to its compatibilizing effect, and showed a clear increase in resistance to break and detachment upon addition of GPTMS. The incorporation of GPTMS to TEOS containing formulations allowed to prepare non-detachable coatings.

Acknowledgements

The authors would like to thank MINECO (MAT2014-53706-C03-01, MAT2014-53706-C03-02) and Generalitat de Catalunya (2014-SGR-67) for giving financial support. BASF and Huntsman are acknowledged for kindly providing Lupasol samples and Araldite GY 240, respectively.

References

[1] G. Schottner, Hybrid sol–gel-derived polymers: applications of multifunctional materials, Chem. Mater. 13 (10) (2001) 3422–3435, http://dx.doi.org/10.1021/cm011060m.
[2] P. Judeinstein, C. Sanchez, Hybrid organic–inorganic materials: a land of multidisciplinarity, J. Mater. Chem. 6 (1996) 511–525, http://dx.doi.org/10.1039/JM9960600511.
[3] D. Wang, G.P. Bierwagen, Sol–gel coatings on metals for corrosion protection, Progr. Org. Coat. 64 (4) (2009) 327–338, http://dx.doi.org/10.1016/j.porgcoat.2008.08.010.
[4] S. Liang, N.N. Matthias, S. Gaan, Recent developments in flame retardant polymeric coatings, Prog. Org. Coat. 76 (11) (2013) 1642–1665, http://dx.doi.org/10.1016/j.porgcoat.2013.07.014.

[5] E. Jacquelot, J. Galy, J.-F. Gérard, A. Roche, E. Chevet, E. Fouissac, D. Verchère, Morphology and thermo-mechanical properties of new hybrid coatings based on polyester/melamine resin and pyrogenic silica, Prog. Org. Coat. 66 (1) (2009) 86–92, http://dx.doi.org/10.1016/j.porgcoat.2009.06.005.
[6] S.-W. Kuo, F.-C. Chang, POSS related polymer nanocomposites, Prog. Polym. Sci. 36 (12) (2011) 1649–1696, http://dx.doi.org/10.1016/j.progpolymsci.2011.05.002.
[7] S. Bizet, J. Galy, J.-F. Gérard, Structure–property relationships in organic–inorganic nanomaterials based on methacryl-POSS and dimethacrylate networks, Macromolecules 39 (7) (2006) 2574–2583, http://dx.doi.org/10.1021/ma051574x.
[8] J.C. Brinker, G.W. Scherer, Sol–Gel Science: The Physics and Chemistry of Sol–Gel Processing, Academic Press, New York, 1990.
[9] U. Schubert, N. Huesing, A. Lorenz, Hybrid inorganic–organic materials by sol–gel processing of organofunctional metal alkoxides, Chem. Mater. 7 (11) (1995) 2010–2027, http://dx.doi.org/10.1021/cm00059a007.
[10] J. Wen, G.-L. Wilkes, Organic/inorganic hybrid network materials by the sol–gel approach, Chem. Mater. 8 (8) (1996) 1667–1681, http://dx.doi.org/10.1021/cm9601143.
[11] L. Matějka, O. Dukh, B. Meissner, D. Hlavatá, J. Brus, A. Strachota, Block copolymer organic–inorganic networks. Formation and structure ordering, Macromolecules 36 (21) (2003) 7977–7985, http://dx.doi.org/10.1021/ma034234p.
[12] H. Beneš, J. Galy, J.-F. Gérard, J. Pleštil, L. Valette, Solvent-free synthesis of reactive inorganic precursors for preparation of organic/inorganic hybrid materials, J. Sol–Gel Sci. Technol. 59 (2011) 598–612, http://dx.doi.org/10.1007/s10971-011-2534-4.
[13] W.K. Goertzen, X. Sheng, M. Akinc, M.R. Kessler, Rheology and curing kinetics of fumed silica/cyanate ester nanocomposites, Polym. Eng. Sci. 48 (5) (2008) 875–883, http://dx.doi.org/10.1002/pen.21027.
[14] L. Boogh, B. Pettersson, J.-A.E. Månson, Dendritic hyperbranched polymers as tougheners for epoxy resins, Polymer 40 (9) (1999) 2249–2261, http://dx.doi.org/10.1016/S0032-3861(98)00464-9.
[15] D. Ratna, R. Varley, G.P. Simon, Toughening of trifunctional epoxy using an epoxy-functionalized hyperbranched polymer, J. Appl. Polym. Sci. 89 (9) (2003) 2339–2345, http://dx.doi.org/10.1002/app.12059.
[16] G. Xu, W. Shi, M. Gong, F. Yu, J. Feng, Curing behavior and toughening performance of epoxy resins containing hyperbranched polyester, Polym. Adv. Technol. 15 (11) (2004) 639–644, http://dx.doi.org/10.1002/pat.520.
[17] D. Foix, A. Serra, L. Amparore, M. Sangermano, Impact resistance enhancement by adding epoxy ended hyperbranched polyester to DGEBA photocured thermosets, Polymer 53 (15) (2012) 3084–3088, http://dx.doi.org/10.1002/pat.520.
[18] M. Flores, X. Fernández-Francos, F. Ferrando, X. Ramis, A. Serra, Efficient impact resistance improvement of epoxy/anhydride thermosets by adding hyperbranched polyesters partially modified with undecenoyl chains, Polymer 53 (23) (2012) 5232–5241, http://dx.doi.org/10.1002/pat.520.
[19] M. Sangermano, H. El Sayed, B. Voit, Ethoxysilyl-modified hyperbranched polyesters as multifunctional coupling agents for epoxy–silica hybrid coatings, Polymer 52 (10) (2011) 2103–2109, http://dx.doi.org/10.1002/pat.520.
[20] V. Geiser, Y. Leterrier, E.J.-A. Månson, Low-stress hyperbranched polymer/silica nanostructures produced by UV curing, sol/gel processing and nanoimprint lithography, Macromol. Mater. Eng. 297 (2) (2012) 155–166, http://dx.doi.org/10.1002/mame.201100108.
[21] M. Sangermano, M. Messori, M. Martin Galleco, G. Rizza, B. Voit, Scratch resistant tough nanocomposite epoxy coatings based on hyperbranched polyesters, Polymer 50 (24) (2009) 5647–5652, http://dx.doi.org/10.1016/j.polymer.2009.10.009.
[22] Y.-T. Bi, Z.-J. Li, W. Liang, Preparation and characterization of epoxy/SiO_2 nano-composites by cationic photopolymerization and sol–gel process, Polym. Adv. Technol. 25 (2) (2014) 173–178, http://dx.doi.org/10.1002/pat.3219.
[23] T. Nazir, A. Afzal, H.M. Siddiqi, Z. Ahmad, M. Dumon, Thermally and mechanically superior hybrid epoxy–silica polymer films via sol–gel method, Prog. Org. Coat. 69 (1) (2010) 100–106, http://dx.doi.org/10.1016/j.porgcoat.2010.05.012.
[24] L. Mascia, L. Prezzi, B. Haworth, Substantiating the role of phase bicontinuity and interfacial bonding in epoxy–silica nanocomposites, J. Mater. Sci. 41 (4) (2006) 1145–1155, http://dx.doi.org/10.1007/s10853-005-3653-5.
[25] C. Acebo, F. Fernàndez-Francos, M. Messori, X. Ramis, A. Serra, Novel epoxy–silica hybrid coatings by using ethoxysilyl-modified hyperbranched poly(ethylenimine) with improved scratch resistance, Polymer 55 (20) (2014) 5028–5035, http://dx.doi.org/10.1016/j.polymer.2014.08.021.
[26] J.J. Chruściel, E. Leśniak, Modification of epoxy resins with functional silanes, polysiloxanes, silsesquioxanes, silica and silicates, Prog. Polym. Sci. 41 (2015) 67–121, http://dx.doi.org/10.1016/j.progpolymsci.2014.08.001.
[27] H. Beneš, J. Galy, J.-F. Gérard, J. Pleštil, L. Valette, Solvent-free synthesis of reactive inorganic precursors for preparation of organic/inorganic hybrid materials, J. Sol–Gel Sci. Technol. 59 (2011) 598–612, http://dx.doi.org/10.1007/s10971-011-2534-4.
[28] L. Matejka, O. Dukh, J. Brus, W.J. Simonsick Jr., B. Meissner, Cage-like structure formation during sol–gel polymerization of glycidyloxypropyl trimethoxysilane, J. Non-Cryst. Solids 270 (2000) 34–47, http://dx.doi.org/10.1016/S0022-3093(00)00074-0.
[29] F. Piscitelli, M. Lavorgna, G.G. Buonocore, L. Verdolotti, J. Galy, L. Mascia, Plasticizing and reinforcing features of siloxane domains in amine-cured epoxy/silica hybrids, Macromol. Mater. Eng. 298 (2013) 896–909, http://dx.doi.org/10.1002/mame.201200222.
[30] M.S. Heise, G.C. Martin, Curing mechanism and thermal properties of epoxy–imidazole systems, Macromolecules 22 (1989) 99–104, http://dx.doi.org/10.1021/ma00191a020.
[31] X. Fernandez-Francos, D. Santiago, F. Ferrando, X. Ramis, J.M. Salla, À. Serra, M. Sangermano, Network structure and thermomechanical properties of hybrid DGEBA networks cured with 1-methylimidazole and hyperbranched poly(ethyleneimine)s, J. Polym. Sci., Part B: Polym. Phys. 50 (21) (2012) 1489–1503, http://dx.doi.org/10.1002/polb.23145.
[32] X. Fernandez-Francos, Theoretical modeling of the effect of proton donors and regeneration reactions in the network build-up of epoxy thermosets using tertiary amines as initiators, Eur. Polym. J. 55 (2014) 35–47, http://dx.doi.org/10.1016/j.eurpolymj.2014.03.022.
[33] S. Ponyrko, L. Kobera, J. Brus, L. Matejka, Epoxy–silica hybrids by nonaqueous sol–gel process, Polymer 54 (2013) 6271–6282, http://dx.doi.org/10.1016/j.polymer.2013.09.034.
[34] Y. Sun, Z. Zhang, K. Moon, C.P. Wong, Glass transition and relaxation behavior of epoxy nanocomposites, J. Polym. Sci., Part B: Polym. Phys. 42 (2004) 3849–3858, http://dx.doi.org/10.1002/polb.20251.
[35] Y. Ni, S. Zheng, Nanostructured thermosets from epoxy resin and an organic–inorganic amphiphile, Macromolecules 40 (2007) 7009–7018, http://dx.doi.org/10.1021/ma0709351.
[36] M. Sangermano, E. Gaspari, L. Vescovo, M. Messori, Enhancement of scratch-resistance properties of methacrylated UV-cured coatings, Prog. Org. Coat. 72 (2011) 287–291, http://dx.doi.org/10.1016/j.porgcoat.2011.04.018.
[37] M. Sangermano, M. Messori, Scratch resistance enhancement of polymer coatings, Macromol. Mater. Eng. 295 (2010) 603–612, http://dx.doi.org/10.1002/mame.201000025.